

# A new algorithm for Upscaling and Short-term forecasting of wind power using Ensemble forecasts

Corinna Möhrlen and Jess U. Jørgensen

*Abstract--* Weather dependent renewable energy sources and especially wind power are frequently the cause of imbalances on the electrical grid. In order to ease the integration of wind and reduce the balance cost it is therefore necessary to estimate how much energy is produced in the following hours. Most power systems have online data on a subset of the renewable energy sources as it is typically not enforced to send frequent reports from all smaller distributed energy sources. Consequently the operator has an incomplete picture of the actual generation. State-of-the-art methodologies combine measurements and forecasts to generate a state estimate. However, the weather forecast often suggests a different state than the online measurements indicate. A first order approximation to the problem is to find a forecast that resembles the online measurement and then trust in this forecast for the next hours. Practical experience however shows that one cannot always find such a matching forecast even within a large ensemble of forecasts. Nevertheless, it is possible to feed the online estimate together with calibrated forecasts into an algorithm, which adapts the model state to fully match the online measurements. The resulting model state is then used as a starting point for the short term forecast covering the next 12 hours. The proposed algorithm computes so-called quality indices of a spatial transformation and coupling in time with the help of all available ensemble forecasts. The methodology is equally applicable to variables with low and high variability. It is designed to support forecast updates several times per minute to capture rapid changes in the weather development that may have impact on the power system.

*Index Terms--* Short-term Wind Power Forecasting, Upscaling methodologies, Data assimilation, Ensemble Kalman Filter, Ensemble predictions.

## I. INTRODUCTION

There exist various approaches of data assimilation in meteorology to adapt numerical weather model states to measurements ([1], [2]). These are variational methods such as the 3DVAR (e.g. [3], [4]) and 4DVAR methods (e.g. [5], [6]), sequential methods such as the

optimal interpolation (OI) (e.g. [1], [7]) and Kalman Filter methods (e.g. [8], [9], [10]). In the variational data assimilation methods (3DVAR, 4DVAR), predefined cost functions that measure the difference between model output and observations are minimised over a discrete time interval. In the sequential data assimilation techniques (OI), the model solution is recursively updated during a forward integration with weights on observations and model output according to their corresponding uncertainties.

These uncertainties are static and based on predefined model output statistics and hence lack the dynamical and non-linear behaviour of the weather and model system.

The Kalman filter methods have therefore gained popularity, because they account for the dynamic propagation of model errors. Anderson and Anderson [11] found an ensemble Kalman filter methodology to combine data assimilation with generation of ensembles to also account for the uncertainty in the forecasting step. However, the method only worked well in low-order systems and could not be applied to large atmospheric models.

In fact it has been found that the sample size of practical ensembles are often too small for atmospheric models to give a meaningful statistics of the distribution of observations in the model state when applying traditional Kalman filter techniques ([8],[9]). Later a number of extensions to the traditional Kalman filter and the ensemble Kalman filter technique were published, which tried to avoid the closure problem of the error covariance evolution when used for large problem sizes or too small ensembles by applying an extended solution ([12], [13]), an adjustment solution ([14]) and also sequential solutions of the filter ([15],[23]).

The limitation of the Kalman filter technique (KF) in meteorological context may however not be a limitation in wind power context, because there the area of observational distribution is rather small, even if the area spans over an entire country. Most of the data used in meteorology are sparse in time but widespread over the entire globe. Nevertheless, if the traditional KF should be applied for a data assimilation task in a wind power context, where the true state of the atmosphere is the target, this would imply that the models would have to generate forecasts in a small area, which is undesired, or it would require unrealistically many computing resources and observational input of meteorological variables.

---

C. Möhrlen is director and co-founder of WEPROG GmbH, Eschenweg 8, 71155 Altdorf, Germany, (e-mail:com@weprog.de).

J. U. Jørgensen is director and co-founder of WEPROG ApS, Aahaven 5, 5631 Ebberup, Denmark (e-mail: juj@weprog.com).

Therefore, only a type of ensemble Kalman filter techniques (EnKF) can be adopted for wind power purposes. As described by Anderson and Anderson [11] and Houtekamer and Mitchell [15], the standard KF propagates the error covariance from one assimilation step to the next, which is computationally expensive.

In the EnKF, this procedure is approximated by using an ensemble of short-range forecasts, where the forecast error covariance is directly computed from the ensemble when they are needed for the data assimilation.

One problem, which has been identified in the ensemble Kalman filter is that the requirement of perturbing the observations to build the ensemble members, the non-linear relationship between analysis-error covariance estimate and the background error covariance estimate can however lead to so-called inbreeding effects ([8],[9],[16]).

In other words, if the ensemble mean error in a data assimilation cycle increases too much, the ensemble spread is no longer representative or appropriate [18,19].

A number of suboptimal ensemble Kalman filter approaches have been developed to overcome this phenomena, e.g. [16],[17], [18], [19]. However, all these approaches are based on the generation of ensemble members with some kind of statistical perturbation.

Meng and Zhang ([19]) found that it was beneficial to use a multi-scheme ensemble approach rather than a single-scheme approach, because it does not require such a large ensemble size to cover the uncertainties. They built an ensemble based on a Penn-State University WRF model kernel and different parameterisation schemes.

We will follow here the same strategy and use an ensemble that is independent of the data assimilation system and also built upon a multi-scheme approach (hereafter named MSEPS). The MSEPS system has 75 ensemble members with various different parameterisation schemes for the advection and the fast physical processes such as condensation and vertical diffusion. The principles of the MSEPS are described in detail in [27]. The spread in the MSEPS is physically based, because all members in the ensemble are essentially equally valid descriptions of the physical properties in the atmosphere and full-scale NWP models.

We want to now investigate how we can generate physically consistent state estimates and forecasts for the electrical power system. Unlike most meteorological measurements there is a continuous inflow of actual measurements on second basis in the power systems. Those measurements are mostly exact, but may not be consistent with the actual meteorological state for a number of reasons. The inconsistency could be caused by operating problems on a number of wind turbines as an example. The meteorological inconsistency can be assumed to follow persistence with good approximation, whereas the weather itself can not. For this reason new state estimates and forecasts are required with frequent updates. As mentioned above, high resolution 3D modelling requires significant computing resources and therefore it is not feasible to conduct a new state estimate

and forecast simulation every minute. Nevertheless, our goal is to be able to issue a new short-term forecast every minute. Therefore, our strategy is to invert all the meteorological ensemble forecasts to match all individually incoming wind power generation data and also any local weather measurements.

Then, we formulate a filter, which will utilize the ensemble forecasts valid at the measurement points to generate a state estimate and a forecast as a one-step process. Our measurement space is in that case a subset of our model space, although we cannot expect there are measurements from every wind generator.

We will show that the methodology has the capability to fully trust measurements and reproduce the impact of them in the following hours with the help of ensemble forecasts. This is a fundamental constraint in the algorithm that measurements must be trusted unless something is technically wrong, i.e. the measurements have not passed the quality control. In fact, the "must trust" constraint is crucial in wind power context, because our aim is to make the model reproduce the real world with the help of modelled results and not vice versa. This is opposite to what is commonly understood as the target in data assimilation in meteorology, where the model state must rather fit the average of the measurement within each model grid point instead of the individual measurements.

Our new methodology broadcasts all measurements in a non-dimensional relative ensemble space to all other model points in our multi-dimensional model space. The signals are filtered on each model point with help of an ensemble forecast covariance matrix.

For this reason we will refer to the new algorithm as an inverted Ensemble Kalman Filter (iEnKF) although the approach is somewhat different from the described EnKF methodologies used in meteorology.

However, the methodology does produce complete multi-dimensional model states. In fact, the main difference lies in the emphasis on the state estimate's sum of the wind generation and the corresponding forecast, rather than the individual grid point.

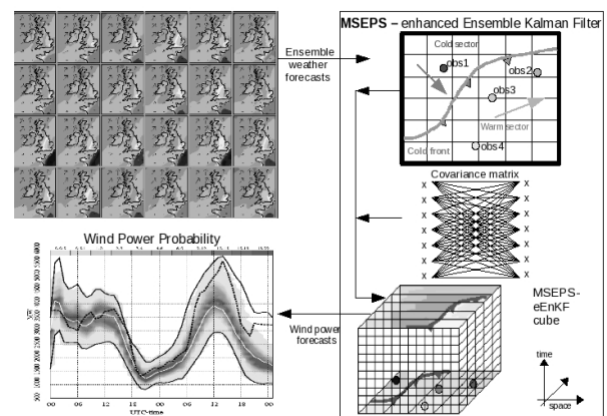


Fig. 1 Flow diagram and principle of the inverted Ensemble Kalman Filter (iEnKF) based on MSEPS forecasts.

Fig. 1 shows a flow diagram of the process of how a weather situation (figure on the right top) is translated into a the forecasting covariance matrix with the ensemble data (left upper figure), and further how the influence of the observations are distributed over the area in each ensemble members space (cube on the right bottom) and then translated into a probabilistic time-series of power production (figure left bottom).

## II. FORMULATION OF THE FILTER

The MSEPS based inverted Ensemble Kalman Filter algorithm (hereafter abbreviated “iEnKF”) we propose here is developed to serve as an operational data assimilation and short-term methodology that can be executed at the same time-resolution as measurements are available, i.e. every minute, if required.

This is achieved by using pre-calculated ensemble forecast data for individual wind farms from the 75 member MSEPS ensemble data set and various available measurements. The pre-calculated values are all calibrated to fit the local measurements to take account for the terrain and local conditions. The other input is measurements from recent hours. In the first step, we form the observation vector  $X$  of absolute values (superscript  $o$  of observation and subscript  $p$  to indicate that it is physical) and  $n$  elements:

$$X_p^o = [x_1, x_2, x_3 \dots x_n] \quad (1)$$

In order to use the different variables, the observation vector has to be transformed into probability space. We do this by introducing an observation operator  $H$ .

The observation operator transfers the physical values into relative, normalised values, now with subscript  $r$ :

$$X_r^o = H \cdot X_p^o \quad (2)$$

where the elements in the observation operator  $H$  are dependent on the sign of the elements in the forecast covariance matrix  $C$  defined below. The assimilated analysis vector can then be formed as

$$X_r^a = A \cdot |C| \cdot X_r^o \quad (3)$$

where  $A$  represents a normalisation and localisation filter and  $C$  the numerical forecast covariance matrix. The final step in the analysis is to transfer the vector back into absolute physical values (subscript  $p$ ) with the help of the observation operator  $H$ :

$$X_p^a = \hat{H} \cdot X_r^a \quad (4)$$

To form the forecast covariance matrix, we need to first form a forecast matrix  $F$ , which in physical space is at least 4-dimensional, as it contains information about each ensemble member, time, location of measurements and variables.

For simplifications we formulate  $F$  as a  $(n \times m)$  matrix, which is built up of columns of ensemble members (dimension  $m$ )

and where  $n$  is the product of time, location and variable dimensions. The time is in 5, 10 or 15 minute resolution and the variables are typically wind power, wind speed and temperature.

$$F = \begin{bmatrix} x_{1,1} & x_{1,2} & \dots & x_{1,m} \\ x_{2,1} & x_{2,2} & \dots & x_{2,m} \\ \dots & \dots & \dots & \dots \\ x_{n,1} & x_{n,2} & \dots & x_{n,m} \end{bmatrix} \quad (5)$$

The forecast covariance matrix  $C$  is then constructed from  $F$  by building correlations between different rows.  $C$  is therefore a symmetric  $(n \times n)$  matrix, where the diagonal is 1. Note that the correlations of the rows are here not in time, but ensemble members. Additionally, the use of correlations between the rows of  $F$  is necessary, because we deal with different variables.

$$C(a,b) = \begin{pmatrix} \begin{bmatrix} F(a,1) \\ F(a,2) \\ \dots \\ F(a,m) \end{bmatrix} & \begin{bmatrix} F(b,1) \\ F(b,2) \\ \dots \\ F(b,m) \end{bmatrix} \end{pmatrix} \quad (6)$$

where  $a, b$  represent different rows in the forecast matrix  $F$ .

## III. PHYSICAL EXPLANATION OF THE FORECAST COVARIANCE MATRIX

To understand what the elements in the forecast covariance matrix  $C$  mean, we can consider a sharp cold front with a short lasting strong wind (see Fig. 2). We assume that the wind measured at the location “ $a$ ” in matrix  $C$  is strong.

We also assume that the ensemble shows a pattern where some members predict the front too early and some members too late, some members too weak or even too strong. Note, that all members in  $F$  are calibrated, thus the members can essentially over-predict the local wind.

The algorithm now searches for the elements in row “ $a$ ” of  $C$  with the highest values. If there is a wind farm, which has been predicted to or is about to develop the strong wind, the algorithm will find that location from the high correlation value in the covariance matrix  $C$ , because the same forecast structure is present at this point.

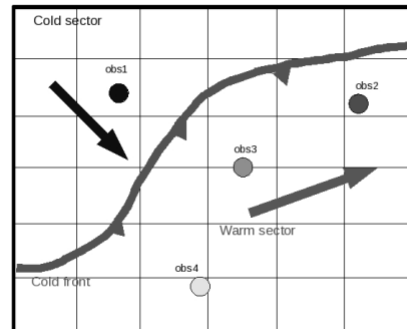


Fig. 2. Conceptual demonstration of the measurement influence on the forecast process.

It may also find other points (wind farms) further downstream with a high correlation, although the cold front may change structure and the covariance elements may indicate that the similarity is not so certain further downstream.

The word "similarity" is in fact a key word in this process, because we use the C matrix to find similar uncertainty patterns and the more similar or anti-similar they are, the more influence point "a" should have on point "b". It is interesting to note that anti-similarity does allow for influence. It is only if there is no similarity that the algorithm blocks the influence between a and b (Fig. 2).

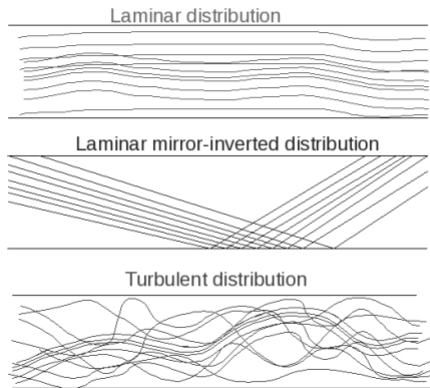


Fig. 3 Ensemble flow pattern between two states. Let row "a" correspond to the left state and row "b" to the right state. The upper figure has covariance value 1, because no line cross another. The middle figure has a mirror inverted distribution and has covariance -1. The lower figure has approximately zero covariance, as there is no pattern between left and right.

A high similarity translates to a laminar flow of the ensemble forecasts from "a" to "b" whereas no similarity corresponds to a chaotic turbulent pattern of the ensemble member connecting lines between "a" and "b" (see Fig. 3).

Consider the case, where the SCADA system of one wind farm (b) is down, but the farm is still operating; there are no weather reports either, but other wind farms are reporting. If we now want to know how much this wind farm is likely to produce, we look at all reporting "a" elements in column "b" of C. Those elements closest to 1 or -1 have most influence. In that way we can estimate the output of the wind farm.

The anti-similar pattern means that all ensemble connections cross each other systematically. This is in fact also the way the approach corrects for phase errors.

An example for such anti-similarity could be the case when all ensemble members are parallel, but show a different phase (see Fig. 3). Let us now take the extreme case, where one member is correct and all others too early on a peak value. During the ramp up, the ensemble minimum or a forecast close to it will be correct and during the ramp down, a maximum forecast or one close to it will be the correct forecast.

Note, that all members will be anti-similar during up-ramps and down-ramps and the members will cross each other, when they peak. Therefore, it is possible to correct the phase in events, where the wind is ramping up in such a way that the correction remains valid also in the down-ramp.

This strategy is of significant value, where phase errors of extremes are responsible for the largest forecasting errors.

Another example of anti-similarity is the ability to transfer influence between different variables, such as wind and pressure. The more developed a low pressure system is, the stronger the wind at some other place. Thus, a low value of measured pressure at location "a" will result in a tendency to believe in high values of wind speed at "b", where the corresponding pressure gradient is found ideally with a strong negative  $C(a,b)$ . This expresses that the C elements can be used in an intelligent way in the computation and distribution of measurement influence.

In a real world problem all measurements provide some influence, because the C elements are not purely -1, 0 or 1, but anything in between. Nevertheless, it is helpful to illustrate how the sign of C determines the H operator used to transform the physical observations to an internal relative non-dimensional variable.

#### IV. PHYSICAL EXPLANATION OF THE H OPERATORS

The H operator is illustrated on Fig. 4. The physical variable is assigned to a relative number between the minimum and maximum of the ensemble. This relative number is defined to apply, where the C elements are positive and the opposite applies where the C elements are negative. In this way all observed values are assigned to a relative number. Elements with zero C value will not contribute in the summation of contribution and are therefore ignored.

The various observational points (wind farms) have different power curves and may stand more or less good at a particular wind direction. Therefore, measurements have to be transformed into a relative model space ranging between the ensemble minimum and maximum using the density of the ensemble forecasts.

We will refer to this relative space as percentile space. However, a more general formulation is required, because the ensemble spread may not always be sufficient to cover the measured value, which will be ignored here for simplicity.

Fig. 5 illustrates how we transform one measurement to all rows in F in equation 3. Suppose that 20% of all ensemble forecasts lie above the measurement and 80% below the current measurement as indicated on Fig. 4. In this case the 80% percentile is defined as the true state and the percentile value is defined by the relative number of ensemble members below that threshold value.

If matrix element  $C(a,b)$  indicates full similarity (e.g.,  $C(a,b)=1.0$ ) then this means that the percentiles distribution is the same at a and b. If the percentile value is 80 at a, then it is also 80 at b. This may however correspond to another physical value, depending on the type of observation at that location. While we invert the percentile value at b, we use the long-term statistical history at a and b that was used to build the power curve.

Similar considerations apply for non-unity positive C values, while negative C values mean that the chosen percentile is constructed by counting from maximum to minimum instead. The use of percentiles for this transformation implies that the bias is assumed homogeneous in percentile space for systems with only one measurement. Localization is required in large systems and also statistical factors to increase responsiveness of the system, which allows the algorithm to also be tuned to different targets.

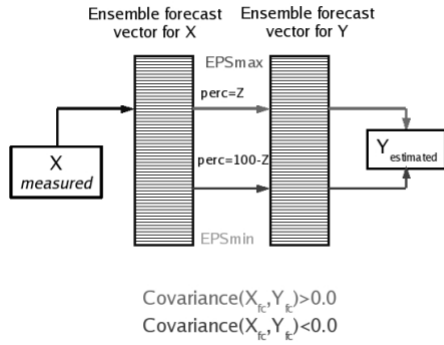


Fig. 4 Example illustration of how the H operator transforms measured values (X) into relative percentile space and further to Y. H selects between two different transformations dependent on the sign of the forecast covariance between variable X and Y.

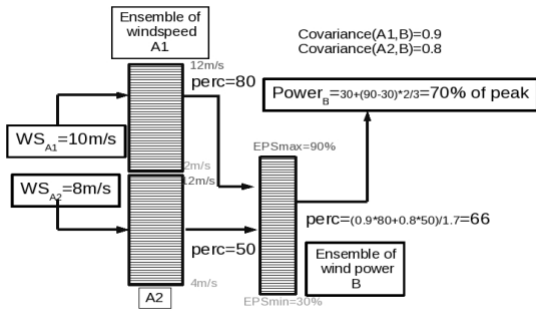


Fig. 5 Illustration of the accumulation and normalization in Eq. 4 with 2 measurements (A1 and A2) having influence on B.

## V. EXPERIMENT

The new algorithm has been tested in a number of areas. However, confidentiality of single wind farm measurements requires making the results anonymous.

Therefore, we have constructed an experiment in an area where many observations were available and selected a random number of the measurement sites as reference measurements and a larger number of measurement sites as the total area capacity.

In our experiment we simulate an area with approximately 80 measurement points, where 20 measurement points have been used to verify the new algorithm's capabilities for upscaling and short-term forecasting to the total of the 80 sites. Fig. 6 shows the distribution of the reference points within the model grid on the left and the total amount of available measurement sites within the model grid on the right figure.

We used 6 months of 15min power production data and the corresponding MSEPS ensemble weather data for the experiment, starting in January and ending in July.

The ensemble weather data resulted in 300 forecast variables for each forecast run, which is the result of 4 different wind speeds times 75 NWP ensemble forecasts. These forecasts are trained with historical data and statistically weighted dependent on their performance.

Additionally, other weather parameters are used to generate power curves according to a number of weather classes. The combination of historical statistics and current weather condition with a so-called probabilistic multi-trend filter (PMT-Filter, [27]) is the basis of the "raw" forecast used to verify the new algorithm in the short-term from 0 to 12h.

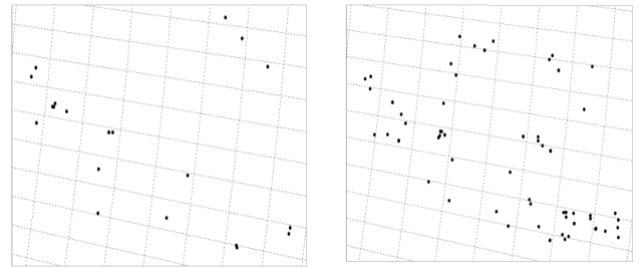


Fig. 6 Distribution of measurement sites in the model grid. The 20 reference sites are shown on the figure to the left, the other 60 sites are shown on the figure to the right.

The computation and later verification of the forecasted total capacity is done by forecasting for the 80 sites and summing them up to a total aggregated value. Additionally, the individual forecasts at the 20 reference sites are used to carry out a data assimilation (upscaling) to the total forecasted production with the iEnKF approach. The persistence forecast is computed with the historic real production data. Although this is to the disadvantage of the forecast in the verification process, it enables to verify data assimilation (upscaling) and forecasting capabilities in one step and in each forecast sequence.

The result then provides the real error of the forecast and assimilation. It also means that in a real-time environment, where only the "upscaled" production and the balance/imbalance on the grid is known, the persistence forecast would have the value of the upscaled online production and the improvement from the forecasts would look somewhat higher.

In this experiment, each forecast sequence had a 4 hour data window, where the forecast can be considered in "assimilation-mode" or "upscaling-mode". The upscaling phase is also used to adopt the forecasts to the measurements in the current weather situation by "filling" the F matrix.

## VI. RESULTS AND DISCUSSION OF THE EXPERIMENT

The verification of the experiment has been carried out with normalised values. Therefore, all following results and error measures are to be understood as “percent of installed capacity” when referred to as percent.

Table 1 shows that the mean load (load factor) in the period January to July of the experiment was 30%. Both the raw MSEPS forecast and the iEnKF forecast shows an average bias in the first 12 hours of approximately 1%.

The verification of the assimilation window showed an assimilation error of the “upscaled” area aggregate from the new algorithm in terms of mean absolute error (MAE) of 2.2% and a root mean square error (RMSE) of 2.9% over the 6 months. This result is quite encouraging (see Table 1).

TABLE I  
SUMMARY OF THE STATISTICS OF THE 6-MONTH EXPERIMENT  
FROM JANUARY AND JULY.

| fcl | mean | eEnKF forecast |     |      | raw forecast |     |      | persistence |      |      |
|-----|------|----------------|-----|------|--------------|-----|------|-------------|------|------|
|     |      | bias           | mae | rmse | bias         | mae | rmse | bias        | mae  | rmse |
| -3  | 29.9 | 1.3            | 2.2 | 2.9  | 1.3          | 5.1 | 6.8  | 0.0         | 0.0  | 0.0  |
| -2  | 29.9 | 1.3            | 2.2 | 2.9  | 1.2          | 5.1 | 6.9  | 0.0         | 0.0  | 0.0  |
| -1  | 29.9 | 1.2            | 2.2 | 2.9  | 1.1          | 5.2 | 7.0  | 0.0         | 0.0  | 0.0  |
| 0   | 29.8 | 1.2            | 2.2 | 3.0  | 1.1          | 5.2 | 7.1  | 0.0         | 0.0  | 0.0  |
| 1   | 29.8 | 1.0            | 2.6 | 3.6  | 1.1          | 5.3 | 7.2  | -0.9        | 2.0  | 6.8  |
| 2   | 29.8 | 1.2            | 3.6 | 5.0  | 1.1          | 5.4 | 7.3  | -1.9        | 4.8  | 10.3 |
| 3   | 29.8 | 1.3            | 4.3 | 5.8  | 1.2          | 5.5 | 7.4  | -2.4        | 6.6  | 12.0 |
| 4   | 29.8 | 1.3            | 4.7 | 6.4  | 1.2          | 5.6 | 7.5  | -2.8        | 8.2  | 13.5 |
| 5   | 29.8 | 1.3            | 5.0 | 6.8  | 1.3          | 5.7 | 7.6  | -3.1        | 9.4  | 14.7 |
| 6   | 29.9 | 1.2            | 5.2 | 7.1  | 1.3          | 5.7 | 7.7  | -3.4        | 10.5 | 15.9 |
| 7   | 29.9 | 1.2            | 5.4 | 7.3  | 1.2          | 5.8 | 7.9  | -3.7        | 11.5 | 17.1 |
| 8   | 29.9 | 1.1            | 5.5 | 7.6  | 1.2          | 5.8 | 8.0  | -3.9        | 12.4 | 18.2 |
| 9   | 29.9 | 1.0            | 5.6 | 7.8  | 1.1          | 5.9 | 8.1  | -4.1        | 13.2 | 19.0 |
| 10  | 29.8 | 1.0            | 5.6 | 7.9  | 1.1          | 5.9 | 8.2  | -4.3        | 13.9 | 19.9 |
| 11  | 29.8 | 0.9            | 5.7 | 8.1  | 1.0          | 6.0 | 8.3  | -4.4        | 14.5 | 20.5 |
| 12  | 29.8 | 0.8            | 5.8 | 8.2  | 1.0          | 6.0 | 8.4  | -4.5        | 15.0 | 21.2 |
| 13  | 29.8 | 0.8            | 5.8 | 8.3  | 0.9          | 6.1 | 8.5  | -4.5        | 15.2 | 21.4 |

In the following hours, it was found that the iEnKF approach is only slightly worse than the persistence forecast in the MAE in the first hour (2.6% against 2.0%), while it is already significantly better than persistence measured in RMSE (3.6% against 6.8%).

The persistence forecast is approaching the raw MSEPS forecast measured in MAE shortly after 2 hours, where the error of the persistence forecast grows from 5% to 6%, while the raw forecast stays under 6% MAE until 12 hours ahead. The persistence forecast reaches an MAE of 15% after 12 hours. Measured in RMSE, the persistence forecast already approaches the raw forecast after one hour, with 6.8% against 7.2% RMSE, respectively. After 2 hours, the persistence reaches an RMSE of 10% and grows relatively fast up to an error of 21% while both the iEnKF and the raw forecast lie under 8.5%.

Fig. 7a and Fig. 7b summarise the results of the 6-month experiment graphically. The fast error growth of the persistence forecast in both MAE and RMSE indicates that the measurements in average do not have a long influence horizon in time, unless some intelligence is used to interpret the measurements.

This is conform with the assumptions made in the development of the iEnKF, i.e. that the influence radius of measurements are dependent of the current weather situation.

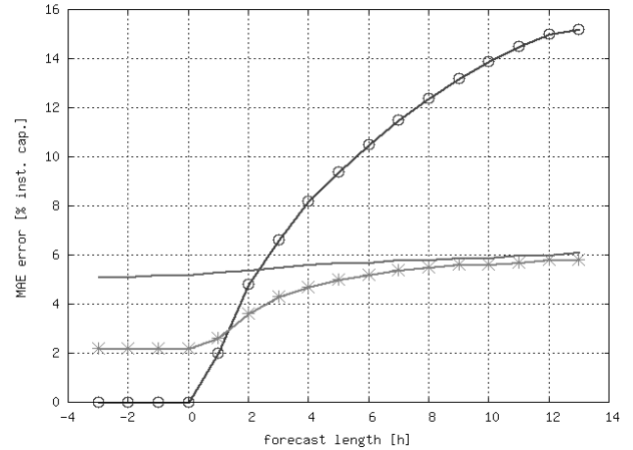


Fig. 7a MAE error statistics for 3-month short-term forecasting test of the iEnKF algorithm. The solid line displays the raw forecast, the solid line with stars displays the MSEPS iEnKF-forecast and the solid line with circles displays persistence.

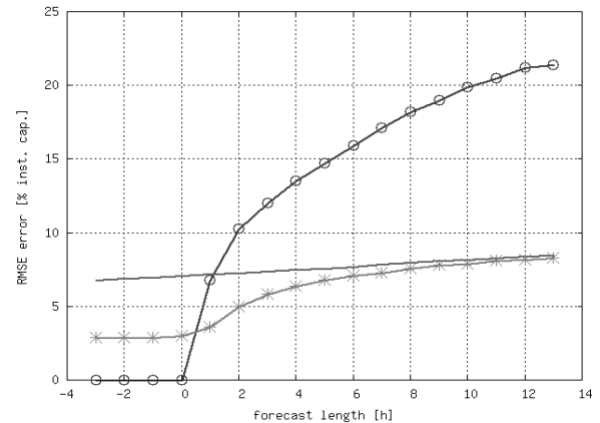


Fig. 7b RMSE error statistics for 3-month short-term forecasting test of the iEnKF algorithm. The solid line displays the raw forecast, the solid line with stars displays the MSEPS iEnKF-forecast and the solid line with circles displays persistence.

It is well known that wind farms are mostly built in areas, where the terrain is complex (coastal or mountainous) and the average wind conditions are above the mean of the surrounding areas. Such conditions imply that measurements have neither long lasting spatial nor temporal influence. Therefore, it is necessary to use an algorithm that can spread the influence of observations dependent on the current weather situation.

Because some measurements have a wide and long lasting radius of influence and others a rather small and short lasting influence on the total production in a given area, traditional methodologies of “upscaling” with only distance measures are insufficient.

While the distance remains an important factor when building up the covariance matrix which defines how and when the influence of a measurement in an area is distributed, the actual weather cannot be neglected, as illustrated in Fig.1.

## VII. THE USE OF DIFFERENT TYPES OF MEASUREMENTS

The proposed iEnKF approach is not only flexible, but also intelligent, because the input ensemble contains the required combination of historical calibration, actual and historic weather and a transformation method for the use of different types of measurements. The percentile method enables the construction of a uniform covariance matrix and in fact ensures that measurements are handled consistent without the need of any physical considerations of their compatibility or irreversibility inside the iEnKF itself.

If the target is to achieve a feedback mechanism for all kinds of data that are in any kind of relation to wind power data, which by default is not reversible, the solution requires a unified methodology to measure the value of an observation and its impact on the total system. This is a well known problem in meteorology, which is extensively researched, because more and more sophisticated observational instrumentation is developed and deployed that require transformations of observations into the numerical weather prediction systems as described e.g. in [18], [19], [20], [21] and [22].

Modern Doppler radar measurements for example require retrieval transformation algorithms, where wind fields are computed with continuity equations and the thermodynamic properties through physical constraints, once the wind field is known. Snyder and Zhang [21] and Zhang et al. [22] discovered that the ensemble Kalman filter is a practical approach for the generation of state estimates with convective-scale data assimilation from such Doppler radar measurements.

The iEnKF introduced in this paper in combination with an ensemble forecast follows in principle these new developments in data assimilation methodologies and hence provides a future compatible and extendible solution with the combination of meteorological and wind power observations and also opens the door for major improvements and reliability enhancements in the short-term forecasting and data assimilation of wind power.

## VIII. CONCLUSIONS

Making use of a meteorological data assimilation technology such as the ensemble Kalman filter technique and translating this into a wind power context does not only solve the problem of distribution of observations in space, but also in time.

By taking the weather situation into account, the well-known timing problem (phase errors) and temporal influence of measurements can be solved mathematically with the help of a forecast covariance matrix.

The additional feature of making use of situations with anti-correlation adds to the physical correctness of the approach, as it identifies, where the borders or in meteorological context fronts are in space and time.

This feature is an important factor, especially, if large wind farms are located in a relatively small area, where sharp fronts pass over the area and where there is risk for cut-off or situations of rapid decrease of power production over short times. Such situations are for example reported regularly in Alberta, Canada, at the foothills of the Rocky Mountains.

We have shown the capabilities of an inverted Ensemble Kalman Filter approach (iEnKF) in this paper designed for short-term wind energy forecasting, upscaling and data assimilation.

The presented approach has been tested in a number of areas and its capabilities demonstrated in a 6-month experiment with a reasonable amount of measurements, typical for a TSO area with a reasonable amount of wind power on the grid. While the algorithm has so far only been tested with wind and wind power measurements, it in fact is future compatible and extendible, as it allows any kind of measurements that is in any kind of relation to the target parameter wind power to be used and mixed into the matrices.

Hence, it is the first physically consistent methodology, where meteorological ensemble forecasts provide the framework for the distribution of observational influence and where it is possible to back-scale aggregated total production measures of an area physically consistent for the statistical training of wind power forecasts. In that sense the iEnKF provides an indirect feedback mechanism to the NWP input for the generation of power curves.

This is a milestone in wind energy forecasting and will be of great value for the large-scale integration and requirements of reliable handling of wind power for transmission system operators, and also for traders and wind farm operators in the electricity markets with fast growing wind capacity and liberalised market rules.

## IX. ACKNOWLEDGMENT

The authors gratefully acknowledge research funds from the Danish PSO-FORSKEL 2006-2008 and the availability of observational data and many fruitful discussions with customers expressing their needs and requirements.

## X. REFERENCES

### *Journal Publications:*

- [1] Dey, C.H., 1989: Evolution of objective analysis methods of NMC's Medium-Range Model, *Wea. Forecasting*, 4, 391-400.
- [2] Ide, K., Courtier, P., Ghil, M, Lorenc, A.C., Unified Notation for Data Assimilation: Perational, Sequential Variational, *J. Met. Soc. Japan*, Special Issue on "Data Assimilation in Meteorology and Oceanography: Theory and practice", Vol. 75, No. 1B, pp 181-189, 1997.

- [3] Courtier, P., E. Andersson, W. Heckley, J. Pailleux, D. Vasiljevic, M. Hamrud, A. Hollingsworth, F. Rabier and M. Fisher, 1998: The ECMWF implementation of three-dimensional variational assimilation (3D-Var). Part 1: formulation. *Quart. J. Roy. Meteor. Soc.*, **124**, 1783-1807.
- [4] Wu, W.-S., R. J. Purser, and D. F. Parrish, 2002: Three dimensional variational analysis with spatially inhomogeneous covariance. *Mon. Wea. Rev.* **130**, 2905-2916.
- [5] Courtier, P. Thepaut, JN, Hollingsworth, A., 1994: A strategy for operational implementation of 4D-Var, using an incremental approach, *Quart. J. Roy. Meteor. Soc.*, **120**, pp. 1367-1387
- [6] Zupanski, D., 1997: A General Weak Constraint Applicable to Operational 4DVAR Data Assimilation Systems. *Mon. Wea. Rev.*, **125**, 2274–2292
- [7] Kanamitsu, M., 1989: Description of the NMC Global Data Assimilation and Forecast System. *Wea. Forecasting*, **4**, 335–342.
- [8] Houtekamer P. L., and H. L. Mitchell, 1998: Data assimilation using an ensemble Kalman filter technique. *Mon. Wea. Rev.*, **126**, 796–811.
- [9] van Leeuwen P. J., 1999: Comments on “Data assimilation using an ensemble Kalman filter technique.”. *Mon. Wea. Rev.*, **127**, 1374–1377.
- [10] Burgers, G., P. Jan van Leeuwen, and G. Evensen, 1998: Analysis Scheme in the Ensemble Kalman Filter. *Mon. Wea. Rev.*, **126**, 1719–1724.
- [11] Anderson J. L., and S. L. Anderson, 1999: A Monte Carlo implementation of the nonlinear filtering problem to produce ensemble assimilations and forecasts. *Mon. Wea. Rev.*, **127**, 2741–2758
- [12] Evensen, G., 1994: Sequential data assimilation with a nonlinear quasi-geostrophic model using Monte Carlo methods to forecast error statistics. *J. Geophys. Res.*, **99** (C5), pp. 10143–10162..
- [13] Todling, R., S.E. Cohn, and N.S. Sivakumaran, 1998: Suboptimal Schemes for Retrospective Data Assimilation Based on the Fixed-Lag Kalman Smoother. *Mon. Wea. Rev.*, **126**, 2274–2286.
- [14] Anderson, J.L., 2001: An ensemble adjustment Kalman Filter, *Mon. Wea. Rev.*, vol 129, issue 12 , pp 2884-2903.
- [15] Houtekamer, P.L., and H.L. Mitchell, 2001: A Sequential Ensemble Kalman Filter for Atmospheric Data Assimilation. *Mon. Wea. Rev.*, **129**, 123–137.
- [16] Bishop, C.H., B.J. Etherton, and S.J. Majumdar, 2001: Adaptive Sampling with the Ensemble Transform Kalman Filter. Part I: Theoretical Aspects. *Mon. Wea. Rev.*, **129**, 420–436.
- [17] Whitaker, J.S., and T.M. Hamill, 2002: Ensemble Data Assimilation without Perturbed Observations. *Mon. Wea. Rev.*, **130**, 1913–1924.
- [18] Houtekamer, P.L., H.L. Mitchell, G. Pellerin, M. Buehner, M. Charron, L. Spacek, and B. Hansen, 2005: Atmospheric Data Assimilation with an Ensemble Kalman Filter: Results with Real Observations. *Mon. Wea. Rev.*, **133**, 604–620.
- [19] Hamill, T.M., and C. Snyder, 2002: Using Improved Background-Error Covariances from an Ensemble Kalman Filter for Adaptive Observations. *Mon. Wea. Rev.*, **130**, 1552–1572.
- [20] Meng, Z., and F. Zhang, 2008: Tests of an Ensemble Kalman Filter for Mesoscale and Regional-Scale Data Assimilation. Part III: Comparison with 3DVAR in a Real-Data Case Study. *Mon. Wea. Rev.*, **136**, 522–540.
- [21] Snyder, C., and F. Zhang, 2003: Assimilation of simulated Doppler radar observations with an ensemble Kalman filter. *Monthly Weather Review*, **131**, 1663-1677.
- [22] Zhang, F., C. Snyder, and J. Sun, 2004: Impacts of initial estimate and observation availability on convective-scale data assimilation with an ensemble Kalman filter. *Monthly Weather Review*, **132**, 1238-1253.
- [23] D. Simon, Sequential Kalman filtering, in “Optimal State Estimation”, New York: Wiley & Sons, ISBN 9780471708582, Online ISBN: 9780470045343, 2006.

#### Dissertations:

- [24] Moehrlen, C, "Uncertainty in Wind Energy Forecasting," Ph.D. dissertation, Dept. Civil & Environmental Eng., Nat. Univ. Ireland, Cork, 2004.

## XI. BIOGRAPHIES

**Corinna Möhrlein** holds a MEngSc degree in Civil Engineering from Ruhr-University of Bochum, Germany (1997) and the University College Cork (UCC), Ireland (1998) and a PhD from UCC (2004). Corinna started her career in the wind energy area in 2000, where she was responsible for the development of wind energy forecasting in Ireland at UCC. From 2001 she began intense studies on ensemble forecasting. In 2003 she founded WEPROG together with Jess U. Jørgensen and concentrates since on the operation and further development of the Multi-Scheme Ensemble prediction System (MSEPS) that today contains 75 ensemble members and is forecasting world wide up to 6 days ahead.

**Jess U. Jørgensen** holds a MSc degree in Geophysics with specialisation in Dynamic Meteorology from Copenhagen University (1989). Already while studying he started his career in the Danish Meteorological Institute (DMI) in 1988. From 1992 to 2002 he was responsible for the operational HIRLAM forecasting system in DMI. Jess was involved in research on wind power forecasting since the early 1990'ies and also coordinated the EU 5<sup>th</sup> Framework project HONEYMOON ([www.honeymoon-windpower.net](http://www.honeymoon-windpower.net)). Jess is co-founder of WEPROG (2003) and concentrates since 2004 on the operation and development of WEPROG's Multi-Scheme Ensemble Prediction System (MSEPS) that today contains 75 ensemble members and is forecasting world wide up to 6 days ahead.

#### Books: